

New rare-earth intermetallic phases $R_3(\text{Fe},\text{M})_{29}\text{X}_n$: ($R=\text{Ce}, \text{Pr}, \text{Nd}, \text{Sm}, \text{Gd}$; $M=\text{Ti}, \text{V}, \text{Cr}, \text{Mn}$; and $X=\text{H}, \text{N}, \text{C}$) (invited)

J. M. Cadogan and Hong-Shuo Li

School of Physics, The University of New South Wales, Sydney NSW 2052, Australia

A. Margarian

Department of Applied Physics, University of Technology, Sydney NSW 2007 and CSIRO Division of Applied Physics, Lindfield NSW 2070, Australia

J. B. Dunlop

CSIRO Division of Applied Physics, Lindfield NSW 2070, Australia

D. H. Ryan

Department of Physics, McGill University, Montréal, Québec H3A 2T8, Canada

S. J. Collocott

CSIRO Division of Applied Physics, Lindfield NSW 2070, Australia

R. L. Davis

Australian Nuclear Science and Technology Organisation, Lucas Heights NSW 2234, Australia

New rare-earth (R), iron-rich ternary intermetallic compounds of the form $R_3(\text{Fe},\text{M})_{29}$ with the monoclinic $\text{Nd}_3(\text{Fe},\text{Ti})_{29}$ structure (space group $P2_1/c$, #14, $Z=2$) have recently been shown to form with $R=\text{Ce}, \text{Nd}, \text{Pr}, \text{Sm},$ and Gd , and $M=\text{Ti}, \text{V}, \text{Cr},$ and Mn . This novel structure is derived from the alternate stacking of $\text{Th}_2\text{Zn}_{17}$ and ThMn_{12} -type segments and contains two R sites and fifteen Fe(M) sites. Reported Curie temperatures of the 3:29 compounds range from 296 K ($R=\text{Ce}, M=\text{Cr}$) to 524 K ($R=\text{Sm}, M=\text{V}$). The 3:29 compounds all show improved magnetic properties after interstitial modification with H or N; in particular, room-temperature coercivity has been reported in $\text{Sm}_3(\text{Fe},\text{Ti})_{29}\text{N}_5$, making this compound a candidate for possible permanent-magnet applications. In this article we will review the work carried out to date on the 3:29 compounds.

The past ten years have witnessed a renewed interest in the structural and magnetic properties of rare-earth (R), iron-rich intermetallic compounds. These intermetallics often show potential for application as permanent-magnet materials, as in the case of $\text{Nd}_2\text{Fe}_{14}\text{B}$, and much effort has been devoted to the search for intermetallic systems whose magnetic properties might surpass those of $\text{Nd}_2\text{Fe}_{14}\text{B}$, which is limited in application by its comparatively low Curie temperature.¹ Two families of intermetallics, the rhombohedral $R_2(\text{Fe},\text{M})_{17}$ and tetragonal $R(\text{Fe},\text{M})_{12}$ compounds, have received special attention since they are both able to absorb N and C as interstitial atoms, with remarkable improvements in their magnetic properties resulting. In fact, $\text{Sm}_2\text{Fe}_{17}\text{N}_{3-\delta}$ and $\text{Nd}(\text{Fe},\text{Ti})_{12}\text{N}_{1-\delta}$ both have uniaxial anisotropy and Curie temperatures over 700 K.

As early as 1990, Jang and Stadelmaier² demonstrated that the tetragonal $\text{NdFe}_{11}\text{Ti}$ phase is unstable at temperatures below about 1000 °C, decomposing into $\text{Nd}_2(\text{Fe},\text{Ti})_{17}$, Fe_2Ti , and $\alpha\text{-Fe}(\text{Ti})$, a fact missed by many workers. In 1992, whilst studying the conditions of formation of $\text{NdFe}_{11}\text{Ti}$, with a view to preparing single-phase material for subsequent nitrogenation and ultimately $\text{NdFe}_{11}\text{TiN}_{1-\delta}$ -based permanent magnets, Collocott *et al.*³ reported the formation of a new high-temperature phase in the Fe-rich corner of the Nd-Fe-Ti ternary phase diagram (see also Margarian *et al.*⁴). The new structure was given as $\text{Nd}_2(\text{Fe},\text{Ti})_{19}$ by Collocott *et al.*³ and its x-ray diffraction (XRD) pattern was in-

dexed on the basis of a (2a,4c) superstructure of the hexagonal TbCu_7 structure. The $\text{Nd}_2(\text{Fe},\text{Ti})_{19}$ compound had a rather low Curie temperature of 411 K but absorption of nitrogen gave a roughly 50% increase in Curie temperature. However, the easy direction of magnetization is in the basal plane (referred to the underlying hexagonal TbCu_7 cell) for both the parent and nitride compounds, precluding its use as a permanent magnet.

There are a number of reports of Sm-Fe-Ti and Nd-Fe-Ti phases at around the same composition as the $\text{Nd}_2(\text{Fe},\text{Ti})_{19}$ compound of Collocott *et al.*³ For example, Saito *et al.*⁵ and Ohashi *et al.*⁶ both observed a transformation from a tetragonal ThMn_{12} structure to a disordered hexagonal TbCu_7 structure in rapidly quenched $\text{SmFe}_{11}\text{Ti}$ as the quenching rate increased. Similarly, Katter *et al.*⁷ observed a transformation from the rhombohedral $\text{Th}_2\text{Zn}_{17}$ structure to the TbCu_7 structure in Sm-Fe alloys around the 1:9 composition, and Neiva *et al.*⁸ reported the formation of a 1:7 phase with composition $\text{Sm}(\text{Fe},\text{Ti})_9$. Jang and Stadelmaier² reported a Ti-stabilized NdFe_7 phase in as-cast alloys. At the same conference at which Collocott *et al.* reported the formation of the $\text{Nd}_2(\text{Fe},\text{Ti})_{19}$ phase,³ Hirose *et al.*⁹ reported the formation of a $\text{Nd}(\text{Fe},\text{Ti})_9$ phase with the TbCu_7 structure during a study of the formation of the ThMn_{12} -type $\text{NdFe}_{11}\text{Ti}$ phase. A common feature of many of these reports is the transformation from the 2:17 or 1:12 structures to the disordered 1:7

structure by rapid solidification with increasing quenching rate.

At the 38th Annual MMM Conference in Minneapolis in November 1993, Cadogan *et al.*¹⁰ reported that the new $\text{Nd}_2(\text{Fe,Ti})_{19}$ structure is monoclinic with a cell derived from that of TbCu_7 . At the same conference, Li *et al.*¹¹ reported the observation of a $\text{Pr}_2(\text{Fe,Ti})_{19}$ phase in a study of the $(\text{Pr}_{1-x}\text{Ti}_x)\text{Fe}_5$ compounds. During discussions at the MMM Conference we learned that the General Motors group (Fuerst *et al.*) had also observed the formation of a new structure in samples of the form $\text{NdFe}_{9.5-x}\text{M}_x$ ($x=0.5$ for $\text{M}=\text{Ti}$, 1.5 for $\text{M}=\text{Cr}$ and $x>3.5$ for $\text{M}=\text{Mn}$) with virtually identical XRD patterns to that of our $\text{Nd}_2(\text{Fe,Ti})_{19}$ sample.^{3,10} Fuerst *et al.*¹² were the first to suggest that the new phase belongs to the $\text{P2}_1/\text{c}$ space group, which was later confirmed by x-ray¹³ and neutron¹⁴ powder diffraction work. The structural determinations^{13,14} also showed that the stoichiometry previously referred to as $\text{Nd}_2(\text{Fe,Ti})_{19}$ is in fact $\text{Nd}_3(\text{Fe,Ti})_{29}$. The $\text{R}_3(\text{Fe,Ti})_{29}$ phase is now known to form with $\text{R}=\text{Sm}$,¹⁵ Pr ,¹¹ Ce ,¹⁶ and Gd ,¹⁷ in addition to $\text{R}=\text{Nd}$.

In this article we shall review the structural and magnetic properties of the new $\text{R}_3(\text{Fe,M})_{29}$ phases.

In the original paper by Collocott *et al.*³ the new Nd-Fe-Ti phase was denoted $\text{Nd}_2(\text{Fe,Ti})_{19}$ and found to form with high-temperature annealing (1100 °C). This structure only forms for a Ti content in the range 3.8–5.1 at. % and was indexed as a (2a,4c) superlattice of the hexagonal TbCu_7 structure. Earlier work by Ivanova, Shcherbakova, and co-workers^{18,19} also showed evidence of a new structure in the $\text{R}_2(\text{Fe}_{0.91}\text{V}_{0.09})_{17}$ ($\text{R}=\text{Y}$, Nd , Sm , and Gd) compounds and these workers described the crystal cell as being a (5a,5c) superlattice of the hexagonal CaCu_5 structure for $\text{R}=\text{Y}$ and a distorted orthorhombic variant of the hexagonal CaCu_5 structure for $\text{R}=\text{Nd}$, Sm , and Gd . The similarities between the XRD patterns of the $\text{Sm}_2(\text{Fe}_{0.91}\text{V}_{0.09})_{17}$ sample of Shcherbakova *et al.*¹⁹ and the $\text{Nd}_2(\text{Fe,Ti})_{19}$ sample of Collocott *et al.*³ strongly suggest that these samples in fact have the same crystal structure.

The structure of $\text{Nd}_2(\text{Fe,Ti})_{19}$ was reported as monoclinic by Cadogan *et al.*¹⁰ and Fuerst *et al.*,¹² the latter group suggesting the $\text{P2}_1/\text{c}$ space group and also that the crystal cell contained six $\text{NdFe}_{9.5-x}\text{M}_x$ units, on the basis of density measurements.

The final structural refinement was obtained from x-ray powder diffraction work by Li *et al.*¹³ who confirmed the monoclinic $\text{P2}_1/\text{c}$ space group and showed that the correct stoichiometry of the new phase is $\text{Nd}_3(\text{Fe,Ti})_{29}$ with two formula units per cell. The 3:29 stoichiometry represents a difference of 1.7% from the original 2:19 stoichiometry. At the same time, Yelon and co-workers¹⁴ refined the 3:29 structure by neutron powder diffraction, and there is excellent agreement between these two structural refinements. In Fig. 1 we show the powder XRD patterns ($\text{CuK}\alpha$ radiation) of $\text{Nd}_3(\text{Fe,Ti})_{29}$, together with those of $\text{Nd}_2(\text{Fe,Ti})_{17}$ and $\text{Nd}(\text{Fe,Ti})_{12}$ for comparison, and in Fig. 2 we show the crystal structure of $\text{Nd}_3(\text{Fe,Ti})_{29}$ (courtesy of Hu and Yelon¹⁴).

The structure of $\text{Nd}_3(\text{Fe,Ti})_{29}$ is intermediate between the well-known rhombohedral $\text{Th}_2\text{Zn}_{17}$ and tetragonal ThMn_{12} structures. The common feature of all these structures is that

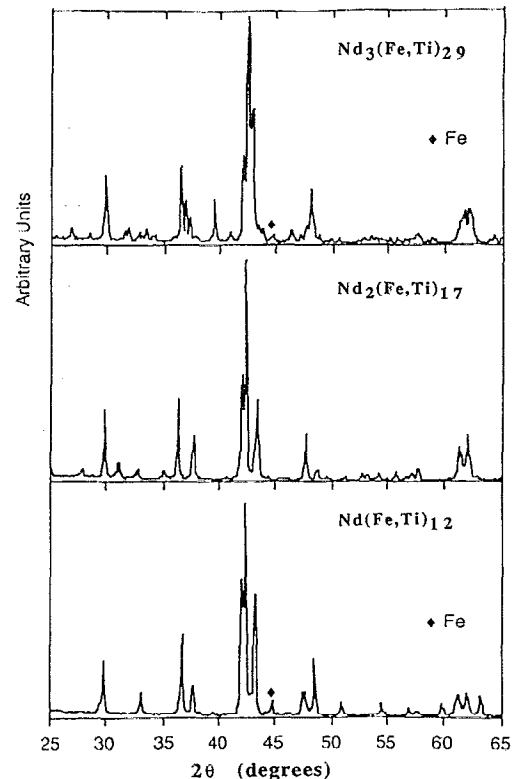
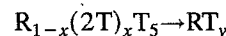


FIG. 1. X-ray powder diffraction patterns ($\text{CuK}\alpha$) of monoclinic $\text{Nd}_3(\text{Fe,Ti})_{29}$, rhombohedral $\text{Nd}_2(\text{Fe,Ti})_{17}$ and tetragonal $\text{Nd}(\text{Fe,Ti})_{12}$.

they are formed by the replacement of R atoms by T-T “dumb-bells” in the hexagonal RT_5 structure. This process may be described by the equation



with the 2:17 structure corresponding to a $\frac{1}{3}$ replacement and the 1:12 structure corresponding to a $\frac{1}{2}$ replacement. The new 3:29 structure corresponds to a $\frac{2}{3}$ replacement and is formed by the alternate stacking of 2:17 and 1:12 segments, in the

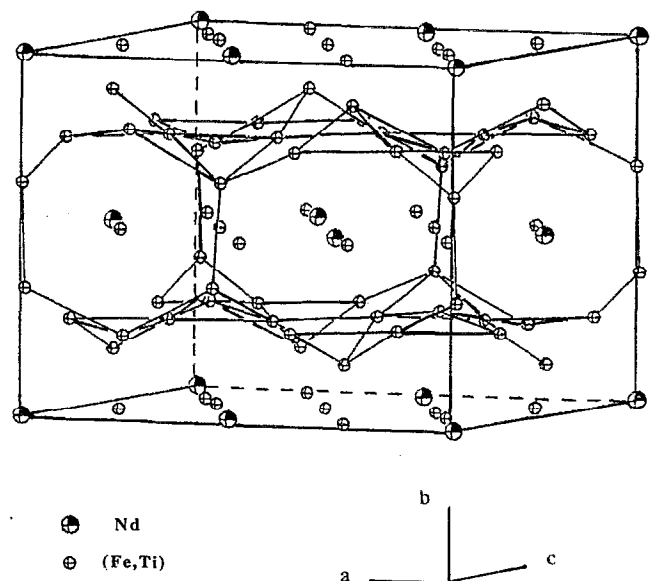


FIG. 2. Monoclinic unit cell of $\text{Nd}_3(\text{Fe,Ti})_{29}$ (Ref. 14).

TABLE I. Lattice parameters and indexation cells used in the analysis of x-ray and neutron diffraction data on the $R_3(\text{Fe},\text{M})_{29}$ compounds. The atomic content of the M atom is at. % [* The indexation of $\text{Y}_2(\text{Fe},\text{V})_{17}$ by Shcherbakova *et al.*¹⁹ was given in both hexagonal and orthorhombic forms for comparison with their other $\text{R}_2(\text{Fe},\text{V})_{17}$ compounds. The lattice parameter a is therefore determined by $a = b\sqrt{3}$ since Shcherbakova *et al.* indexed $\text{Y}_2(\text{Fe},\text{V})_{17}$ as a true hexagonal structure.]

R	M	at. % M	$a(\text{\AA})$	$b(\text{\AA})$	$c(\text{\AA})$	$\beta(^{\circ})$	Cell	Ref.
Y	V	8.1	24.3	...	20.9	...	hexag.	18
Y	V	8.1	42.09	24.30	20.90	...	ortho-hex	*19
Nd	V	8.1	42.80	24.31	21.04	...	ortho.	19
Sm	V	8.1	42.60	24.27	20.99	...	ortho.	19
Gd	V	8.1	42.45	24.30	20.86	...	ortho.	19
Nd	Ti	4.1	9.88	...	16.96	...	hexag.	3
Nd	Ti	4.1	10.644	8.585	9.755	96.92	mono.	10
Nd	Ti	4.8	10.65	8.59	9.75	96.9	mono.	12,30
Nd	Ti	4.1	10.641	8.5913	9.748	96.928	mono.	13
Nd	Ti	3.9	10.6628	8.6056	9.7610	96.996	mono.	14
Nd	Ti	3.6	10.62	8.58	9.73	96.912	mono.	22
Sm	Ti	6.1	10.65	8.58	9.72	96.98	mono.	15
Sm	Ti	6.3	10.62	8.56	9.72	96.972	mono.	22
Sm	Ti	3.8	10.63	8.57	9.72	97.0	mono.	30
Ce	Ti	5.0	10.56	8.49	9.68	96.7	mono.	30
Pr	Ti	4.5	10.63	8.59	9.74	96.892	mono.	22
Pr	Ti	4.7	10.64	8.63	9.76	97.1	mono.	30
Ce	Cr	12.8	10.53	8.45	9.63	96.8	mono.	30
Nd	Cr	14.3	10.60	8.55	9.71	96.8	mono.	12
Nd	Cr	13.8	10.59	8.56	9.71	96.9	mono.	30
Sm	Cr	14.1	10.56	8.51	9.68	96.9	mono.	30
Nd	Mn	33.3	10.65	8.61	9.75	96.9	mono.	12

ratio 1:1. Such structural relationships were considered by Stadelmaier in 1984,²⁰ who indeed predicted the occurrence of a number of novel structures including the 3:29 structure. Stadelmaier showed that such new structures must have one edge length equal to $a_0\sqrt{3}$ where a_0 is the relevant lattice parameter of the 1:5 cell. Both structural refinements of $\text{Nd}_3(\text{Fe},\text{Ti})_{29}$ (Refs. 13,14) have $b \sim a_0\sqrt{3}$, in agreement with Stadelmaier's criterion. In Table I we give the lattice parameters and indexation cells of the various $\text{R}_3(\text{Fe},\text{M})_{29}$ compounds studied to date.

TABLE II. Atomic positions and lattice parameters of $\text{Nd}_3(\text{Fe}_{0.955}\text{Ti}_{0.045})_{29}$ obtained from the x-ray powder diffraction pattern refinement according to the space group $\text{P}2_1/\text{c}$.¹³

Atom	Site	x	y	z
Nd	2a	0	0	0
Nd	4e	0.5925(4)	0	0.1851(1)
Fe	2d	1/2	1/2	0
Fe	4e ₁	0.8570(5)	1/2	0.2141(1)
Fe	4e ₂	0.2570(5)	1/2	0.0141(1)
Fe	4e ₃	4/5	0.785(1)	1/10
Fe	4e ₄	4/5	0.215(1)	1/10
Fe	4e ₅	0.628(1)	0.638(2)	0.1858(1)
Fe	4e ₆	0.628(1)	0.362(2)	0.1858(1)
Fe	4e ₇	0	0.853(2)	1/2
Fe	4e ₈	0.892(1)	0	0.284(2)
Fe	4e ₉	4/5	1/4	7/20
Fe	4e ₁₀	4/5	3/4	7/20
Fe	4e ₁₁	0.706(1)	1/2	0.411(2)
Fe	4e ₁₂	0.410(2)	3/4	0.072(4)
Fe	4e ₁₃	0.597(2)	3/4	0.444(4)
Fe	4e ₁₄	0	3/4	1/4
$R_p = 8.8\%$		$a = 10.641(1) \text{\AA}$		
$R_{wp} = 11.9\%$		$b = 8.5913(8) \text{\AA}$		
$R_{\text{expt}} = 5.9\%$		$c = 9.748(1) \text{\AA}$		
$R_{\text{Bragg}} = 5.6\%$		$\beta = 96.928(6)^{\circ}$		
		$Z = 2$		

The monoclinic $\text{R}_3(\text{Fe},\text{M})_{29}$ structure contains two R sites (2a and 4e) and fifteen Fe(M) sites (2d and fourteen 4e sites), and in Table II we give the atomic positions of these sites, deduced by Li *et al.*¹³ from x-ray powder diffraction. The relationships between the lattice parameters of the 3:29 and 1:5 structures are

$$a = \sqrt{(2a_0)^2 + (c_0)^2}$$

$$b = \sqrt{3}a_0$$

$$c = \sqrt{(a_0)^2 + (2c_0)^2}$$

$$\beta = \arctan\left(\frac{2a_0}{c_0}\right) + \arctan\left(\frac{a_0}{2c_0}\right),$$

and in Fig. 3 we show the relationship between the 3:29 and 1:7 crystal cells.¹⁰ In Fig. 4 we show a schematic representation of the dumb-bell substitution sequence, projected onto the (110) plane of the CaCu_5 structure, for the 2:17, 3:29, and 1:12 structures.¹³

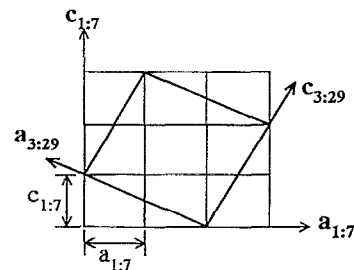


FIG. 3. Crystallographic relationship in the a - c plane between the monoclinic unit cell of $\text{Nd}_3(\text{Fe},\text{Ti})_{29}$ and the hexagonal TbCu_5 cell (Ref. 10).

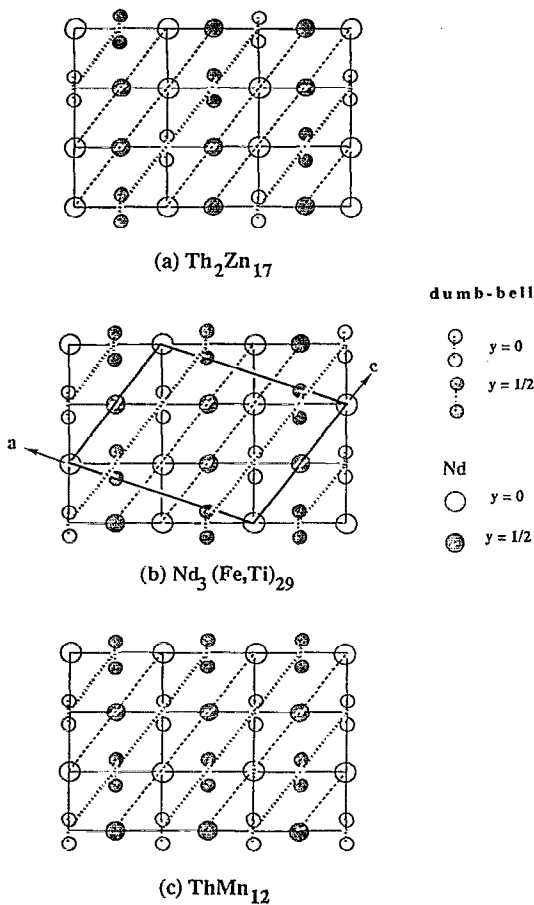


FIG. 4. Schematic representation of the geometrical relationship and the dumb-bell substitution sequence, in a projection onto the (110) plane of the hexagonal CaCu_5 structure for the 3:29, 2:17, and 1:12 structures (Ref. 13).

The rhombohedral 2:17 structure forms with light R atoms by a regular dumb-bell replacement in the 1:5 structure, and we therefore suggest that the new monoclinic 3:29 structure will also form only for light R (including Gd). It is quite

likely that a different structure derived from the stacking of *hexagonal* 2:17 and *tetragonal* 1:12 segments will exist for 3:29 compounds with heavy R atoms. It is also likely that other intermediate phases based on the stacking of the rhombohedral 2:17 and tetragonal 1:12 segments will exist, besides 3:29. For example, a 2:1 stacking ($\frac{2}{3}$ dumb-bell replacement) would correspond to a 5:46 phase, whereas a 1:2 stacking ($\frac{2}{3}$ dumb-bell replacement) would correspond to a 4:41 phase.

Hu and Yelon¹⁴ drew attention in their paper to the fact that the crystal structure of 3:29 shows a distinct stacking along the *b* direction which is reminiscent of the $\text{Nd}_2\text{Fe}_{14}\text{B}$ structure, in that there is an alternating stacking of R-containing and R-free layers. Furthermore, they pointed out that the distinction between the dumb-bell and non-dumb-bell Fe sites is not as clear-cut as in the 2:17 and 1:12 structures, since the 3:29 structure exhibits a number of rather short Fe-Fe bonds ($<2.45 \text{ \AA}$). Taking advantage of the fact that Ti has a negative neutron scattering length, Hu and Yelon demonstrated that the Ti atoms in $\text{Nd}_3(\text{Fe,Ti})_{29}$ occupy sites with a low Nd coordination. In a subsequent paper, Hu and Yelon²¹ presented a comprehensive summary of the bond lengths in $\text{Nd}_3(\text{Fe,Ti})_{29}$ and showed that the distribution in bond length is virtually continuous over the range 2.36–3.01 \AA , in contrast to the $\text{Nd}_2(\text{Fe,Ti})_{17}$ and $\text{Nd}(\text{Fe,Ti})_{12}$ compounds. In their paper, Hu and Yelon also reported the formation of $\text{Nd}_3(\text{Fe,V})_{29}$ and $\text{Nd}_3(\text{Fe,Al})_{29}$, but no structural details were presented.

The $\text{R}_3(\text{Fe,M})_{29}$ compounds are ferromagnetic with Curie temperatures in the range 296 K [$\text{R}=\text{Ce}$, $\text{M}=\text{Cr}$ (Ref. 30)] to 524 K [$\text{R}=\text{Gd}$, $\text{M}=\text{V}$ (Ref. 19)]. XRD experiments on magnetically aligned powder samples of $\text{Nd}_3(\text{Fe,Ti})_{29}$ (Ref. 22) and $\text{Sm}_3(\text{Fe,Ti})_{29}$ (Ref. 15) indicate that the easy direction of magnetization is in the *a-b* basal plane (hexagonal description), along [201], whereas the powder neutron diffraction results of Hu and Yelon^{14,21} were interpreted in

TABLE III. Intrinsic magnetic parameters (Curie temperature, saturation magnetization and anisotropy field) of the $\text{R}_3(\text{Fe,M})_{29}$ compounds (*=12 K measurement and \times =77 K measurement).

R	M	at. % M	T_c (K)	$M_{\text{sat}}(4 \text{ K})$ ($\mu_B/\text{f.u.}$)	$M_{\text{sat}}(\text{RT})$ ($\mu_B/\text{f.u.}$)	$B_a(4 \text{ K})$ (T)	$B_a(\text{RT})$ (T)	Ref.
Y	V	8.1	439	41	...	3.8	...	18
Y	V	8.1	439	41	19
Nd	V	8.1	480	50	19
Sm	V	8.1	490	41	...	23.9	17.3	19
Gd	V	8.1	524	24	19
Ce	Ti	5.0	322	47.0	31.4	30
Pr	Ti	4.5	373	56.4*	46.2	6.3*	4.0	22
Pr	Ti	4.7	393	60.7	45.4	30
Nd	Ti	4.1	480	46.3	42.1	3
Nd	Ti	4.1	411	57.3	48.6	10
Nd	Ti	4.8	424	58.9	44.5	12
Nd	Ti	3.9	361	21
Nd	Ti	3.6	396	58.2*	47.6	9.8*	7.7	22
Nd	Ti	4.1	426	26
Nd	Ti	5.0	419	58.5	44.8	30
Sm	Ti	6.1	486	46.0 \times	43.8	15
Sm	Ti	6.3	452	50.8*	43.6	7.8*	5.8	22
Sm	Ti	3.8	469	51.6	45.2	30
Ce	Cr	12.8	296	35.4	30
Nd	Cr	14.3	417	45.0	33.4	12
Nd	Cr	13.8	410	45.3	34.5	30
Sm	Cr	14.1	423	38.6	31.1	30
Nd	Mn	33.3	<295	17.1	12

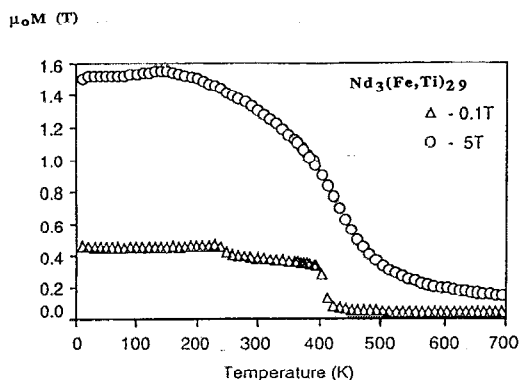


FIG. 5. Magnetization curves for $\text{Nd}_3(\text{Fe,Ti})_{29}$ in applied fields of 0.1 and 5 T (Ref. 10).

terms of the magnetically easy direction being the crystal a -axis at 295 K. The saturation magnetization of $\text{Nd}_3(\text{Fe,Ti})_{29}$ is $58 \mu_B/\text{f.u.}$ at 4 K and $47 \mu_B/\text{f.u.}$ at 295 K, and its anisotropy field $B_a = 7.7$ T at 295 K and 9.8 T at 12 K.^{10,22} In Table III we summarize the intrinsic magnetic properties of the various $\text{R}_3(\text{Fe,M})_{29}$ compounds.

The temperature dependence of the magnetization of $\text{Nd}_3(\text{Fe,Ti})_{29}$ presented by Cadogan *et al.*¹⁰ (Fig. 5) shows clear evidence of a magnetization reorientation around 220 K ($B_{\text{appl}} = 0.1$ T), and recent low-temperature neutron work by Hu and Yelon²¹ confirms a shift in the easy direction of magnetization away from the crystal a axis (at 295 K) to the a - b plane (at 12.5 K). Our analysis of ^{57}Fe average hyperfine fields, deduced from Mössbauer measurements, also supports the occurrence of a spin reorientation at low temperatures.²³ Other evidence of magnetization reorientations in the form of FOMPs (first-order magnetization processes) has been reported by Fuerst *et al.*¹² who observed a FOMP in the magnetization of $\text{NdFe}_{9.0}\text{Ti}_{0.5}$ measured on fixed powders at 5 K; the observed FOMP field is 2.0 T. Yang *et al.*¹⁵ also observed a FOMP in $\text{Sm}_3(\text{Fe,Ti})_{29}$ by singular-point detection measurements; their FOMP fields are 2.2 T at 77 K and 3.0 T at 4 K. The exact nature of the magnetization reorientations in $\text{Nd}_3(\text{Fe,Ti})_{29}$ are as yet unclear.

Finally, Fuerst *et al.*¹² reported that their $\text{NdFe}_{6.0}\text{Mn}_{3.5}$ sample had a coercive field of 3.8 kOe at 5 K, whereas their $\text{NdFe}_{9.0}\text{Ti}_{0.5}$ and $\text{NdFe}_{8.0}\text{Cr}_{1.5}$ samples had coercivities less than 1.2 kOe.

Shcherbakova *et al.*¹⁹ demonstrated that their $\text{R}_2(\text{Fe}_{0.91}\text{V}_{0.09})_{17}$ ($\text{R} = \text{Y, Nd, Sm, and Gd}$) phases all absorb nitrogen with substantial increases in Curie temperature ensuing (see Table IV). Significantly, they also found an easy [001] direction of magnetization (hexagonal description) in $\text{Sm}_2(\text{Fe}_{0.91}\text{V}_{0.09})_{17}\text{N}_{2.5}$ and measured anisotropy fields B_a of 23.9 T at 4 K and 17.3 T at 260 K. The formation of a carbide $\text{Y}_2(\text{Fe}_{0.91}\text{V}_{0.09})_{17}\text{C}_{1.0}$, which had a modest 30 K increase in Curie temperature over the parent phase, was also reported by these authors.

Collocott *et al.*³ showed that $\text{Nd}_3(\text{Fe,Ti})_{29}$ absorbs nitrogen, with a 5.4% increase in volume and a 45% increase in Curie temperature resulting. However, their XRD patterns on magnetically aligned powder samples showed that both the parent and nitride compounds had a - b planar anisotropy.

Yang *et al.*²⁴ reported the formation of $\text{Sm}_3(\text{Fe,Ti})_{29}\text{N}_5$ with a 7.1% volume increase relative to the parent phase. The Curie temperature of the nitride was 750 K compared to 486 K for the parent phase and, importantly, $\text{Sm}_3(\text{Fe,Ti})_{29}\text{N}_5$ shows c -axis anisotropy. The anisotropy field of $\text{Sm}_3(\text{Fe,Ti})_{29}\text{N}_5$ is 18.1 T at 4 K, and Yang *et al.*²⁴ were able to develop a coercivity of $\mu_0 H_c = 1.3$ T at 4 K. Subsequent work by Hu *et al.*²⁵ on ball-milled $\text{Sm}_3(\text{Fe,Ti})_{29}\text{N}_5$ produced a maximum energy product $(BH)_{\text{max}}$ of 105 kJ m^{-3} after ball milling for 4.5 h.

Ryan *et al.*²⁶ have studied the absorption of hydrogen and nitrogen by $\text{Nd}_3(\text{Fe,Ti})_{29}$ using thermopiezic analysis, thermogravimetric analysis (TGA), and ^{57}Fe Mössbauer spectroscopy, and found that the addition of hydrogen leads to a significant increase in Curie temperature but very little change in Fe moment, whereas the addition of nitrogen increases both parameters. Attempts to form a $\text{Nd}_3(\text{Fe,Ti})_{29}\text{C}_x$ carbide were unsuccessful due to disproportionation of the material, although a "magnetic event" was observed by TGA at 660 K which was tentatively assigned to a $\text{Nd}_3(\text{Fe,Ti})_{29}\text{C}_x$ phase.

As mentioned earlier, the 3:29 structure is formed by the 1:1 alternate stacking of 2:17 and 1:12 segments and Li²⁷ has identified the interstitial sites available to N or C atoms in the 3:29 structure by considering the interstitial sites in the 1:12 and 2:17 structures. There are two 4e interstitial sites with the special atomic positions $(\frac{1}{2}\frac{1}{2}\frac{1}{2})$ and $(\frac{1}{2}\frac{1}{4}\frac{1}{4})$, giving a maximum N content of $\text{Nd}_3(\text{Fe,Ti})_{29}\text{N}_4$ according to the relation

TABLE IV. Intrinsic magnetic properties and volume expansions of the $\text{R}_3(\text{Fe,M})_{29}\text{N}_x$ compounds [$\times = 12$ K measurement and * refers to $\text{Nd}_3(\text{Fe,Ti})_{29}\text{H}_x$].

R	M	at. % M	\times	$\Delta V(\%)$	T_c (K)	$M_{\text{sat}}(4 \text{ K})$ ($\mu_B/\text{f.u.}$)	$M_{\text{sat}}(\text{RT})$ ($\mu_B/\text{f.u.}$)	$B_a(4 \text{ K})$ (T)	$B_a(\text{RT})$ (T)	Ref.
Y	V	8.1	4	...	706	19
Nd	V	8.1	4	...	706	19
Sm	V	8.1	4	6	743	19
Gd	V	8.1	4	...	728	19
Nd	Ti	4.1	4	5.4	695	...	57.6	3
Nd	Ti	4.1	4.5	6.5	723	26
Sm	Ti	6.1	5	7.1	750	60.9	53.3	18.1	12.8	24
Nd	Ti	4.1	6.1*	2.2	>548	26
Pr	Ti	4.5	5.4	6.9	700	68.8 \times	63.6	13.9 \times	7.5	22
Nd	Ti	3.6	4.7	5.4	725	61.3 \times	61.7	19.4 \times	8.1	22
Sm	Ti	6.3	3.8	5.3	710	59.4 \times	52.3	14.3 \times	10.7	22

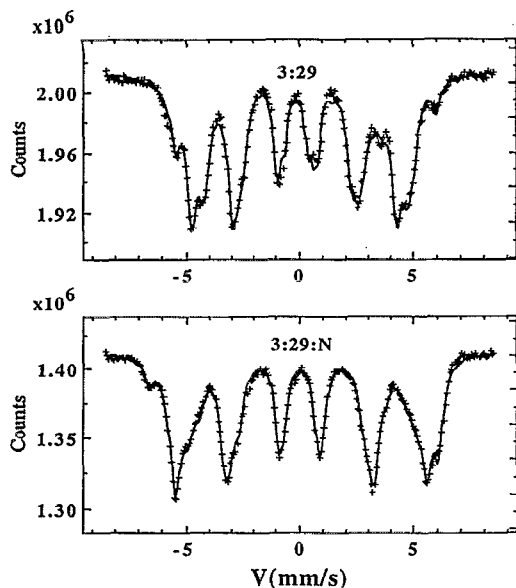
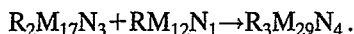


FIG. 6. ^{57}Fe Mössbauer spectra of $\text{Nd}_3(\text{Fe,Ti})_{29}$ and $\text{Nd}_3(\text{Fe,Ti})_{29}\text{N}_{4.5}$ obtained at 12 K with a $^{57}\text{CoRh}$ source (Ref. 26).



Ryan and Cadogan²⁶ calculated the sizes of the holes in the 3:29 structure and found that all holes capable of accommodating interstitial H, N, or C are $4e$ sites. The two largest holes have radii of 0.64 and 0.59 Å and are thus able to accommodate N or C, giving $\text{R}_3\text{M}_{29}\text{X}_4$ as the maximum interstitial X content. The next largest hole has a radius of 0.45 Å, which is too small for N or C but can accommodate H, giving a maximum H content of $\text{R}_3\text{M}_{29}\text{H}_6$, as observed.²⁶

In Table IV we summarize the work on interstitially modified 3:29 compounds. The interstitial contents are approximate values, and we note that the results on the $\text{Sm}_3(\text{Fe,Ti})_{29}$ nitride by Yang *et al.*²⁴ and Hu *et al.*²⁵ give a nitrogen content of N_5 . Ryan *et al.*²⁶ calculated a nitrogen content of $\text{N}_{4.5}$ in $\text{Nd}_3(\text{Fe,Ti})_{29}\text{N}_x$ but caution that such results with $\text{N}_{>4}$ may be due to partial decomposition of the samples.

The room-temperature ^{57}Fe Mössbauer spectra of $\text{Nd}_3(\text{Fe,Ti})_{29}$ and its nitride were presented by Cadogan *et al.*,²⁸ along with spectra of $\text{Nd}_2(\text{Fe,Ti})_{17}$ and $\text{Nd}(\text{Fe,Ti})_{12}$ for comparison. The $\text{Nd}_3(\text{Fe,Ti})_{29}$ phase has an average ^{57}Fe hyperfine field (B_{hf}) of 20.8 T at 295 K which corresponds to an average Fe moment of 1.33 μ_B , assuming a conversion factor of 15.6 T/ μ_B .²⁹ The corresponding $\langle B_{\text{hf}} \rangle$ values of $\text{Nd}_2(\text{Fe,Ti})_{17}$ and $\text{Nd}(\text{Fe,Ti})_{12}$ are 15.4 and 24.8 T, respectively. The $\langle B_{\text{hf}} \rangle$ of $\text{Nd}_3(\text{Fe,Ti})_{29}\text{N}_4$ is 29.6 T at 295 K, the 42% increase in field being attributed to the N-induced increase in Curie temperature of about 200 K. Subsequent low-temperature (12 K) ^{57}Fe Mössbauer studies by Ryan *et al.*²⁶ gave $\langle B_{\text{hf}} \rangle$ values of 29.0 and 33.4 T for $\text{Nd}_3(\text{Fe,Ti})_{29}$ and $\text{Nd}_3(\text{Fe,Ti})_{29}\text{N}_{4.5}$, respectively. The $\langle B_{\text{hf}} \rangle$ values of $\text{Nd}_3(\text{Fe,Ti})_{29}\text{H}_{6.1}$ are 30.2 and 26.4 T at 12 and 295 K, respectively.²⁶ Given the large number of Fe sites in the

$\text{Nd}_3(\text{Fe,Ti})_{29}$ structure (15 sites) and the effects of site occupation by Ti in $\text{Nd}_3(\text{Fe,Ti})_{29}$, one can only deduce the average hyperfine parameters from the Mössbauer spectra, with any certainty. In Fig. 6 we show the ^{57}Fe Mössbauer spectra of $\text{Nd}_3(\text{Fe,Ti})_{29}$ and $\text{Nd}_3(\text{Fe,Ti})_{29}\text{N}_{4.5}$ obtained at 12 K with a $^{57}\text{CoRh}$ source.

Interestingly, a comparison of $\langle B_{\text{hf}} \rangle$ of $\text{Nd}_3(\text{Fe,Ti})_{29}$ at 12 and 295 K (Ref. 26) with saturation magnetization results²² suggests that the low-temperature magnetic structure of $\text{Nd}_3(\text{Fe,Ti})_{29}$ is noncollinear (Cadogan *et al.*²³).

¹J. F. Herbst, Rev. Mod. Phys. **63**, 819 (1991); K. H. J. Buschow, Rep. Prog. Phys. **54**, 1123 (1991).

²T. S. Jang and H. H. Stadelmaier, J. Appl. Phys. **67**, 4957 (1990).

³S. J. Collocott, R. K. Day, J. B. Dunlop, and R. L. Davis, in Proceedings of the Seventh International Symposium on Magnetic Anisotropy and Coercivity in R-T Alloys, Canberra, July 1992, p. 437.

⁴A. Margarian, J. B. Dunlop, R. K. Day, and W. Kalceff (these proceedings).

⁵H. Saito, M. Takahashi, and T. Wakiyama, J. Appl. Phys. **64**, 5965 (1988).

⁶K. Ohashi, R. Osugi, and Y. Tawara, in Proceedings of the Tenth International Workshop on RE Magnets and their Applications, Kyoto, 1989, pp. 13–22.

⁷M. Katter, J. Wecker, and L. Schultz, J. Appl. Phys. **70**, 3188 (1991).

⁸A. C. Neiva, F. P. Missell, B. Grieb, E.-T. Henig, and G. Petzow, J. Less Common Met. **170**, 293 (1991).

⁹S. Hirose, K. Makita, T. Ikegami, and M. Umemoto, Proceedings of the Seventh International Symposium on Magnetic Anisotropy and Coercivity in Rare-Earth Transition Metal Alloys, Canberra, July 1992, pp. 389–402.

¹⁰J. M. Cadogan, H.-S. Li, R. L. Davis, A. Margarian, J. B. Dunlop, and P. B. Gwan, J. Appl. Phys. **75**, 7114 (1994).

¹¹H.-S. Li, Suharyana, J. M. Cadogan, G. J. Bowden, J.-M. Xu, S. X. Dou, and H. K. Liu, J. Appl. Phys. **75**, 7120 (1994).

¹²C. D. Fuerst, F. E. Pinkerton, and J. F. Herbst, J. Magn. Magn. Mater. **129**, L115 (1994).

¹³H.-S. Li, J. M. Cadogan, R. L. Davis, A. Margarian, and J. B. Dunlop, Solid State Commun. **90**, 487 (1994).

¹⁴Z. Hu and W. B. Yelon (unpublished).

¹⁵F.-M. Yang, B. Nasunjilegal, H.-Y. Pan, J.-L. Wang, R.-W. Zhao, B.-P. Hu, Y.-Z. Wang, H.-S. Li, and J. M. Cadogan (unpublished).

¹⁶A. Margarian, J. B. Dunlop, and S. J. Collocott (to be published).

¹⁷J.-M. Xu, H.-S. Li, J. M. Cadogan, S. X. Dou, and H. K. Liu (to be published).

¹⁸G. V. Ivanova, Y. V. Shcherbakova, Y. V. Belozero, A. S. Yermolenko, and Y. I. Teytel, Phys. Met. Metallogr. **70**, 63 (1990).

¹⁹Y. V. Shcherbakova, G. V. Ivanova, A. S. Yermolenko, Y. V. Belozero, and V. S. Gaviko, J. Alloys Compounds **182**, 199 (1992).

²⁰H. H. Stadelmaier, Z. Metallkd. **75**, 227 (1984).

²¹Z. Hu and W. B. Yelon (these proceedings).

²²A. Margarian, J. B. Dunlop, S. J. Collocott, H.-S. Li, J. M. Cadogan, and R. L. Davis, submitted to the Eighth International Symposium on Magnetic Anisotropy and Coercivity in R-T Alloys, Birmingham, September 1994.

²³J. M. Cadogan, D. H. Ryan, A. Margarian, and J. B. Dunlop (to be published).

²⁴F.-M. Yang, B. Nasunjilegal, J.-L. Wang, H.-Y. Pan, W.-D. Qing, R.-W. Zhao, B.-P. Hu, Y.-Z. Wang, G.-C. Liu, H.-S. Li, and J. M. Cadogan (unpublished).

²⁵B.-P. Hu, G.-C. Liu, Y.-Z. Wang, B. Nasunjilegal, R.-W. Zhao, F.-M. Yang, H.-S. Li, and J. M. Cadogan, J. Phys. Condens. Matter **6**, L197 (1994).

²⁶D. H. Ryan, J. M. Cadogan, A. Margarian, and J. B. Dunlop (these proceedings).

²⁷H.-S. Li (private communication).

²⁸J. M. Cadogan, R. K. Day, J. B. Dunlop, and A. Margarian, J. Alloys Compounds **201**, L1 (1993).

²⁹B.-P. Hu, H.-S. Li, and J. M. D. Coey, Hyp. Int. **45**, 233 (1989).

³⁰C. D. Fuerst, F. E. Pinkerton, and J. F. Herbst (these proceedings).